



**HAL**  
open science

## Rush Larsen time stepping methods of high order for stiff problems in cardiac electrophysiology

Yves Coudière, Charlie Douanla Lontsi, Charles Pierre

► **To cite this version:**

Yves Coudière, Charlie Douanla Lontsi, Charles Pierre. Rush Larsen time stepping methods of high order for stiff problems in cardiac electrophysiology. 2017. hal-01557856v1

**HAL Id: hal-01557856**

**<https://hal.science/hal-01557856v1>**

Preprint submitted on 6 Jul 2017 (v1), last revised 11 Jun 2019 (v3)

**HAL** is a multi-disciplinary open access archive for the deposit and dissemination of scientific research documents, whether they are published or not. The documents may come from teaching and research institutions in France or abroad, or from public or private research centers.

L'archive ouverte pluridisciplinaire **HAL**, est destinée au dépôt et à la diffusion de documents scientifiques de niveau recherche, publiés ou non, émanant des établissements d'enseignement et de recherche français ou étrangers, des laboratoires publics ou privés.

# Rush Larsen time stepping methods of high order for stiff problems in cardiac electrophysiology

Y. COUDIÈRE, C. DOUANLA LONTSI, AND C. PIERRE

ABSTRACT. The development of efficient solvers in cardiac electrophysiology requires high order (semi) explicit and stable time stepping methods. In this paper are introduced two new exponential integrators of orders 3 and 4. They generalize the order 2 Rush Larsen scheme derived by Perego and Veneziani [24] in 2009. They have been named Rush Larsen of order  $k$ , shortly  $RL_k$ . The  $RL_k$  schemes are explicit exponential multistep integrators. They display a simple general formulation and an easy implementation.

The  $RL_k$  schemes are shown to be stable under perturbation (or 0-stable) and convergent of order  $k$ . Their Dahlquist stability analysis is performed. They have a very large stability domain provided that the stabilizer associated with the method captures well enough the stiff modes of the problem. The  $RL_k$  method is numerically studied as applied to the membrane equation in cardiac electrophysiology.

## 1. INTRODUCTION

The monodomain model in cardiac electrophysiology [3, 4, 5], formulates as a coupling between an evolution reaction diffusion equation and an ODE system. On the heart domain  $\Omega$  and on the time interval  $[0, T]$ , it reads:

$$(1) \quad \frac{\partial v}{\partial t} = Av + f_1(v, w) + s(x, t), \quad \frac{\partial w}{\partial t} = f_2(v, w),$$

where  $A$  is a diffusion operator. The first unknown  $v : \Omega \times [0, T] \rightarrow \mathbb{R}$  is the cellular transmembrane potential. The second unknown  $w : \Omega \times [0, T] \rightarrow \mathbb{R}^N$  gathers variables describing the cellular membrane state: it incorporates ionic concentrations and gating variables. The source term  $s(x, t)$  allows to apply stimulation currents to the system. The reaction terms  $f_1$  and  $f_2$  are cell membrane models for ionic currents and voltage, that are named ionic models. Ionic models originally have been developed by Hodgkin and Huxley [17] in 1952 for the squid axon. Several

---

*Date:* July the 10<sup>th</sup> 2017.

*2010 Mathematics Subject Classification.* 65L04, 65L06, 65L20, 65L99.

*Key words and phrases.* stiff equations, explicit high-order multistep methods, exponential integrators of Adams type, stability and convergence, Dahlquist stability .

This work was supported by the ANR, INRIA and the CNRS.

ionic models have been especially designed for cardiac cells, such as the Beeler Reuter model [1], the Luo and Rudy models [21, 22] or the TNNP model [27].

Numerical simulations in cardiac electrophysiology face two difficulties. The first one is the stiffness displayed by the solutions of (1). This is commonly coped with by resorting to very fine space and time grids, associated with high computational costs. Stiffness is due to the coexistence of fast and slow variables. Fast variables in ionic models are described by equations in the ODE system in (1) of the form,

$$(2) \quad \frac{\partial w_i}{\partial t} = f_{2,i}(v, w) = a_i(v)w_i + b_i(v).$$

This feature of ionic models will be exploited here. The rate of variations  $a_i(v)$  will be inserted in the numerical method in order to allow stable computations at large time step.

The second difficulty is the nature of the reaction terms  $f_1$  and  $f_2$  in (1). It is non linear and the operation  $(v, w) \rightarrow f_i(v, w)$  has a significant cost. For example, this operation for the TNNP model [27] involves the computation of 50 exponentials. These operations need to be performed at every node of the grid. They represent a large computational load. Their total amount needs to be maintained as low as possible. Fully implicit time stepping methods (that require a non linear solver) therefore are avoided.

Our objective for the numerical resolution of (1) is to go towards high order methods, in order to reduce the grid size. A high order time stepping method is required that fulfills two conditions. It must have strong stability properties. It has to be explicit for the reaction terms. To this aim, we will focus in this paper on the time integration of stiff ODE systems,

$$(3) \quad \frac{dy}{dt} = f(t, y), \quad y(0) = y_0,$$

for which a reformulation of the following kind is available,

$$(4) \quad \frac{dy}{dt} = a(t, y)y + b(t, y), \quad y(0) = y_0.$$

The linear part  $a(t, y)$  will be referred to as the stabilizer. Exponential integrators fulfill these two conditions. We refer to [23, 14, 12] for general reviews. They have been widely studied for the quasilinear equations,  $\partial_t y = Ay + b(t, y)$ , see *e.g.* [13, 7, 11, 16, 28, 20]. The basic idea is to use the exact solution of the linearized equation in order to stabilize the numerical scheme. In general this implies to compute a matrix exponential. This is the supplementary cost associated to exponential integrators.

The targeted problem (4) displays a non constant linear part  $a(t, y)$ . Exponential integrators have been less studied in that case. Exponential integrators of Adams type for a non constant linear part have been first considered by Lee and Preiser

[19] in 1978 and by Chu [2] in 1983. Recently, Ostermann *et al* [15, 18] developed and analyzed the linearized exponential Adams method. The original problem (3) is reformulated after each time step as,

$$\frac{dy}{dt} = J_n y + c_n(t, y), \quad J_n = \partial_y f(t_n, y_n), \quad c_n(t, y) = f(t, y) - J_n y.$$

The Jacobian matrix  $J_n$  is used as a stabilizer. This requires the computation of matrix exponentials. Moreover, when the fast variables of the system are known, stabilization can be performed only on these variables. Considering the full Jacobian as the stabilizer implies unnecessary computational efforts. To avoid these problems, an alternative is to set the stabilizer as a part or as an approximation of the Jacobian. This has been analyzed in [29], [25] and [6] for exponential Rosenbrock, exponential Runge Kutta and exponential Adams type methods respectively. For exponential Adams type methods, equation (4) is reformulated after each time step as,

$$\frac{dy}{dt} = a_n y + c_n(t, y), \quad a_n = a(t_n, y_n), \quad c_n(t, y) = f(t, y) - a_n y.$$

The resulting scheme is (see details in [15, 6]),

$$(5) \quad y_{n+1} = y_n + h [\varphi_1(a_n h) (a_n y_n + \gamma_1) + \varphi_2(a_n h) \gamma_2 + \dots + \varphi_k(a_n h) \gamma_k],$$

where  $\gamma_i$  are the coefficients of the Lagrange interpolation polynomial of  $c_n(t, y)$  (in a classical  $k$ -step setting) and where the functions  $\varphi_j$  are given by,

$$(6) \quad \varphi_0(z) = e^z, \quad \varphi_{j+1}(z) = \frac{\varphi_j(z) - 1/j!}{z}.$$

Independently, Perego and Veneziani [24] presented in 2009 a new exponential integrator of order 2, of a different nature:

$$(7) \quad y_{n+1} = y_n + h \varphi_1(\alpha_n h) (\alpha_n y_n + \beta_n).$$

The two constants  $\alpha_n$  and  $\beta_n$  are updated after each time step. They are defined with  $\alpha_n = 3/2a_n - 1/2a_{n-1}$  and  $\beta_n = 3/2b_n - 1/2b_{n-1}$  with  $a_j = a(t_j, y_j)$  and  $b_j = b(t_j, y_j)$ . The numerical solution  $y_{n+1}$  in (7) satisfies,

$$(8) \quad y_{n+1} = z(t_{n+1}) \quad \text{with} \quad z' = \alpha_n z + \beta_n, \quad z(t_n) = y_n.$$

The ODE (8) involves two constant terms only. It is interesting to obtain the order 2 when approximating the original ODE (4) on  $[t_n, t_{n+1}]$  with that simple ODE (8).

In this paper we will study the general formulation (7). It results in schemes with a very simple definition. It is in particular simpler than the exponential Adams integrators (5). We will show that such schemes also exist at the orders 3 and 4, for an explicit definition of the two constants  $\alpha_n$  and  $\beta_n$ . These schemes will be referred to as Rush Larsen schemes of order  $k$ , shortly denoted  $RL_k$ . They will be shown to be stable under perturbation (or 0-stable) and convergent of order  $k$ . The

Dahlquist stability analysis for the  $RL_k$  schemes is also performed. It is a practical tool that allows to dimension the time step  $h$  with respect to the variations of  $f(t, y)$  in problem (3), see *e.g.* [10]. When considering varying stabilizers, the stability domain depends on how  $f(t, y)y$  is decomposed in equation (4), following [24]. The stability domains are numerically computed and shown to be much larger than in the absence of stabilization (*i.e.* when  $a(t, y) = 0$ ) provided that  $a(t, y)$  captures well enough the variations of  $f(t, y)$ . The performances of the  $RL_k$  method are evaluated for the membrane equation in cardiac electrophysiology. They are compared with the exponential Adams integrators (5). The two methods have a very similar robustness to stiffness. They both allow stable computations on coarse time grids. At large time step, the  $RL_3$  and  $RL_4$  schemes are slightly more accurate, meanwhile with a simpler implementation.

The paper is organized as follows. The  $RL_k$  schemes are derived in section 2 and their numerical analysis is made in sections 2 and 3. The Dahlquist stability analysis is in section 4. The numerical results are presented in section 5. The paper ends with the conclusion section 6.

In the sequel  $h$  denotes the time step and  $t_n = nh$  the associated time instants.

## 2. $RL_k$ SCHEME DEFINITION AND CONSISTENCY

**Definition 1.** The  $RL_k$  scheme is an explicit  $k$ -step method. It is defined with the formulation (7) for the following setting of  $\alpha_n$  and of  $\beta_n$ :

$$\begin{aligned}
 RL_2 : \quad & \alpha_n = \frac{3}{2}a_n - \frac{1}{2}a_{n-1}, \quad \beta_n = \frac{3}{2}b_n - \frac{1}{2}b_{n-1}, \\
 RL_3 : \quad & \alpha_n = \frac{1}{12}(23a_n - 16a_{n-1} + 5a_{n-2}), \\
 & \beta_n = \frac{1}{12}(23b_n - 16b_{n-1} + 5b_{n-2}) + \frac{h}{12}(a_nb_{n-1} - a_{n-1}b_n). \\
 RL_4 : \quad & \alpha_n = \frac{1}{24}(55a_n - 59a_{n-1} + 37a_{n-2} - 9a_{n-3}), \\
 & \beta_n = \frac{1}{24}(55b_n - 59b_{n-1} + 37b_{n-2} - 9b_{n-3}) \\
 & \quad + \frac{h}{12}(a_n(3b_{n-1} - b_{n-2}) - (3a_{n-1} - a_{n-2})b_n),
 \end{aligned}$$

where  $a_j = a(t_j, y_j)$  and  $b_j = b(t_j, y_j)$ .

A solution  $y(t)$  of equation (4) on a time interval  $[0, T]$  is fixed. It is recalled that the scheme (7) is consistent of order  $k$  if:

- being given a time step  $h$  and a time instant  $kh \leq t_n \leq T - h$ ,

- being given the numerical approximation  $y_{n+1}$  in (7) computed with  $y_{n-j} = y(t_{n-j})$  for  $j = 0 \dots k - 1$ ,

we have  $|y_{n+1} - y(t_n + h)| \leq Ch^{k+1}$ , for a constant  $C$  only depending on the problem (4) data  $a, b, y_0$  and on  $T$ .

**Proposition 1.** *Assume that the functions  $a(t, y)$  and  $b(t, y)$  in problem (4) are  $C^k$  regular. Moreover assume that  $a(t, y)$  either is a diagonal matrix or a constant linear operator.*

*Then the  $RL_k$  scheme is consistent of order  $k$ .*

*Remark 1.* In the case of a constant linear part  $a(t, y) = A$ , we always have  $\alpha_n = A$ . The definition of  $\beta_n$  also simplifies at the order 3 and 4,

$$RL_3 : \quad \beta_n = \frac{1}{12}(23b_n - 16b_{n-1} + 5b_{n-2}) - \frac{h}{12}A(b_n - b_{n-1}).$$

$$RL_4 : \quad \beta_n = \frac{1}{24}(55b_n - 59b_{n-1} + 37b_{n-2} - 9b_{n-3}) - \frac{h}{12}A(2b_n - 3b_{n-1} + b_{n-2}).$$

*Remark 2.* The assumption “ $a(t, y)$  either is a diagonal matrix or a constant linear operator” in proposition 1 has the following origin. To analyze the scheme consistency we will derive a Taylor expansion in  $h$  of (7). That series is computed with the help of Taylor expansions in  $h$  for  $\alpha_n$  and  $\beta_n$ .

Assume the simple form  $\alpha_n = \alpha_0 + h\alpha_1$ . We need to expand  $\varphi_1(\alpha_n h)$  as a series in  $h$ . The function  $\varphi_1$  is analytic on  $\mathbb{C}$ . However in the matrix case, the equality,  $\varphi_1(M + N) = \varphi_1(M) + \varphi_1'(M)N + \dots + \varphi_1^{(i)}(M)N^i/i! + \dots$  holds if  $M$  and  $N$  are commutative matrices. Therefore one cannot expand  $\varphi_1(\alpha_n h)$  without the assumptions that  $\alpha_0$  and  $\alpha_1$  are commutative.

That difficulty vanishes if  $a(t, y)$  is constant or scalar or, equivalently, a diagonal matrix.

The proof of proposition 1 is based on the following result.

**Lemma 2.** *With the same assumption as in proposition 1, the scheme (7) is consistent of order  $k$  if:*

$$\begin{aligned}
k = 2 : \quad & \alpha_n = a_n + \frac{1}{2}a'_n h + O(h^2), \quad \beta_n = b_n + \frac{1}{2}b'_n h + O(h^2). \\
k = 3 : \quad & \alpha_n = a_n + \frac{1}{2}a'_n h + \frac{1}{6}a''_n h^2 + O(h^3), \\
& \beta_n = b_n + \frac{1}{2}b'_n h + \frac{1}{12}(a'_n b_n - a_n b'_n)h^2 + O(h^3). \\
k = 4 : \quad & \alpha = a_n + \frac{1}{2}a'_n h + \frac{1}{6}a''_n h^2 + \frac{1}{24}a'''_n h^3 + O(h^4), \\
& \beta = b_n + \frac{1}{2}b'_n h + \frac{1}{12}(a'_n b_n - a_n b'_n)h^2 + \left( \frac{1}{24}b'''_n + \frac{1}{24}(a''_n b_n - a_n b''_n) \right) h^3 + O(h^4).
\end{aligned}$$

Where  $a'_n, a''_n, a'''_n$  and  $b'_n, b''_n, b'''_n$  denote the successive derivatives at time  $t_n$  of the functions  $t \mapsto a(t, y(t))$  and  $t \mapsto b(t, y(t))$ .

*Proof of lemma 2.* By assumption the functions  $a$  and  $b$  in problem (4) are  $C^k$  regular. Therefore a solution  $y$  of problem (4) on a closed time interval  $[0, T]$  is  $C^{k+1}$  regular. Its derivatives up to order  $k+1$  can be bounded by constants only depending on the problem (4) data and on  $T$ . The Taylor expansion of  $y$  at time instant  $t_n$  is,

$$y(t_n + h) = y(t_n) + \sum_{j=1}^k \frac{s_j}{j!} h^j + O(h^{k+1}),$$

with  $s_j = y^{(j)}(t_n)$ . Using that  $y' = ay + b$  we get,

$$\begin{aligned}
s_1 &= a_n y_n + b_n, \\
s_2 &= (a'_n + a_n^2) y_n + a_n b_n + b'_n, \\
s_3 &= (a''_n + 3a_n a'_n + a_n^3) y_n + b''_n + a_n b'_n + 2a'_n b_n + a_n^2 b_n, \\
s_4 &= (a'''_n + 4a''_n a_n + 3a_n'^2 + 6a'_n a_n^2 + a_n^4) y_n \\
&\quad + b'''_n + b''_n a_n + 3a''_n b_n + 5a'_n a_n b_n + 3a'_n b'_n + a_n^3 b_n + a_n^2 b'_n.
\end{aligned}$$

A series expansion in  $h$  for  $\alpha_n$  and for  $\beta_n$  is formally introduced,

$$\begin{aligned}
\alpha_n &= \alpha_{n,0} + \alpha_{n,1} h + \cdots + \alpha_{n,k-1} h^{k-1} + O(h^k), \\
\beta_n &= \beta_{n,0} + \beta_{n,1} h + \cdots + \beta_{n,k-1} h^{k-1} + O(h^k).
\end{aligned}$$

With the assumption that  $a(t, y)$  is either constant or a diagonal matrix (see remark 2), a Taylor expansion of the numerical solution  $y_{n+1}$  in (7) can be performed,

$$y_{n+1} = y(t_n) + \sum_{j=1}^k \frac{r_j}{j!} h^j + O(h^{k+1}).$$

A direct computation of the  $r_j$  gives,

$$r_1 = \alpha_{n,0} y_n + \beta_{n,0},$$

$$r_2 = (2\alpha_{n,1} + \alpha_{n,0}^2) y_n + 2\beta_{n,1} + \alpha_{n,0} \beta_{n,0},$$

$$r_3 = (6\alpha_{n,2} + \alpha_{n,0}^3 + 6\alpha_{n,0} \alpha_{n,1}) y_n + 3\alpha_{n,1} \beta_{n,0} + 6\beta_{n,2} + \alpha_{n,0}^2 \beta_{n,0} + 3\alpha_{n,0} \beta_{n,1},$$

$$r_4 = (24\alpha_{n,0} \alpha_{n,2} + 24\alpha_{n,3} + 12\alpha_{n,1} \alpha_{n,0}^2 + 12\alpha_{n,1}^2 + \alpha_{n,0}^4) y_n \\ + 12\alpha_{n,2} \beta_{n,0} + 24\beta_{n,3} + 12\alpha_{n,0} \beta_{n,2} + 12\alpha_{n,1} \beta_{n,1} + 4\alpha_{n,0}^2 \beta_{n,1} + 8\alpha_{n,0} \alpha_{n,1} \beta_{n,0} + \alpha_{n,0}^3 \beta_{n,0}.$$

The condition to be consistent of order  $k$  is:  $r_i = s_i$  for  $1 \leq i \leq k$ . Lemma 2 consistency conditions are obtained by solving recursively these relations.  $\square$

*Proof of proposition 1.* It is a direct and simple consequence of the backwards differentiation formula, that we first recall. Consider a real function  $f$ , its derivatives can be approximated as follows (with obvious notations). For the first derivative,

$$f'_n = \frac{f_n - f_{n-1}}{h} + O(h), \\ = \frac{1}{2h} (3f_n - 4f_{n-1} + f_{n-2}) + O(h^2), \\ = \frac{1}{6h} (11f_n - 18f_{n-1} + 9f_{n-2} - 2f_{n-3}) + O(h^3).$$

For the second derivative,

$$f''_n = \frac{1}{h^2} (f_n - 2f_{n-1} + f_{n-2}) + O(h), \\ = \frac{1}{h^2} (2f_n - 5f_{n-1} + 4f_{n-2} - f_{n-3}) + O(h^2).$$

For the third derivative,

$$f'''_n = \frac{1}{h^3} (f_n - 3f_{n-1} + 3f_{n-2} - f_{n-3}) + O(h),$$



With these formula, the consistency condition at order 3 on  $\alpha_n$  in lemma 2 becomes,

$$\begin{aligned}\alpha_n &= a_n + \frac{1}{2}a'_n h + \frac{1}{6}a''_n h^2 + O(h^3), \\ &= a_n + \frac{1}{4}(3a_n - 4a_{n-1} + a_{n-2}) + \frac{1}{6}(a_n - 2a_{n-1} + a_{n-2}) + O(h^3) \\ &= \frac{1}{12}(23a_n - 16a_{n-1} + 5a_{n-2}) + O(h^3).\end{aligned}$$

We retrieve the definition of  $\alpha_n$  for the  $RL_3$  scheme. The same holds for  $\beta_n$  and the  $RL_3$  scheme then is consistent order 3.

The proof is the same at the other orders.  $\square$

### 3. STABILITY UNDER PERTURBATION AND CONVERGENCE

We refer to [9, Ch. III-8] for the definitions of convergence and of stability under perturbation (or 0-stability). For the analysis of ODE numerical integrators, it is commonly assumed that  $f$  in (3) is uniformly Lipschitz in its second variable  $y$ . That hypothesis will be replaced by assumptions based on the formulation (4). Precisely it will be assumed that,

$$(9) \quad a(t, y) \text{ is bounded, } a(t, y), b(t, y) \text{ are uniformly Lipschitz in } y.$$

The Lipschitz constants for  $a$  and  $b$  are denoted  $L_a$  and  $L_b$  respectively. The upper bound on  $|a(t, y)|$  is denoted  $M_a$ .

**Proposition 3.** *With the assumptions (9) the  $RL_k$  scheme is stable under perturbation.*

**Corollary 4.** *Assume that  $a(t, y)$  and  $b(t, y)$  are  $C^k$  regular and that  $a(t, y)$  either is a diagonal or a constant matrix. In addition assume (9). Then the  $RL_k$  scheme is convergent of order  $k$ .*

Stability under perturbation together with consistency implies convergence, see e.g. [9] or [6] where the current setting has been detailed. Therefore corollary 4 is an immediate consequence of the propositions 1 and 3. Before to prove the proposition 3 definitions are needed.

Equation (3) is considered on  $E = \mathbb{R}^N$  with the max norm  $|\cdot|$ . A final time  $T > 0$  is considered. The space of  $N \times N$  matrices is equipped with the operator norm  $\|\cdot\|$  associated to  $|\cdot|$ . The space  $E^k$  is equipped with the max norm  $|Y|_\infty = \max_{1 \leq i \leq k} |y_i|$  with  $Y = (y_1, \dots, y_k)$ .

The  $RL_k$  scheme is defined with the mapping,

$$s_{t,h} : Y = (y_1, \dots, y_k) \in E^k \longrightarrow s_{t,h}(Y) \in E,$$

with,

$$s_{t,h} = y_k + h\varphi_1(\alpha_{t,h}(Y)h) (\alpha_{t,h}(Y)y_k + \beta_{t,h}(Y)),$$

in such a way that  $y_{n+1} = s_{t_n,h}(y_{n-k+1}, \dots, y_n)$  in (7). The functions  $\alpha_{t,h}$  and  $\beta_{t,h}$  are given in definition 1. For instance,  $\alpha_{t,h}(Y)$  for the  $RL_3$  scheme reads,

$$\alpha_{t,h}(Y) = \frac{1}{12}(23a(t, y_3) - 16a(t-h, y_2) + 5a(t-2h, y_1)), \quad Y = (y_1, y_2, y_3).$$

A first way to prove the stability under perturbation is to show that  $s_{t,h}$  is globally Lipschitz in  $Y$ . For this the derivative  $\partial_Y s_{t,h}$  has to be analyzed. As developed in the remark 2, this will imply restrictions on  $a(t, y)$ : either diagonal or constant. A second way is to prove the two following stability conditions,

$$(10) \quad |s_{t,h}(Y) - s_{t,h}(Z)| \leq |Y - Z|_\infty (1 + Ch(|Y|_\infty + 1)),$$

$$(11) \quad |s_{t,h}(Y)| \leq |Y|_\infty(1 + Ch) + Ch$$

where  $C$  is a constant only depending on the data  $a, b, y_0$  in equation (4) and on the final time  $T$ . These are sufficient conditions for the stability under perturbation, as proved in [6].

That second way will be used here, for it is more general and giving rise to less computations. The core of the proof is the following property of the  $RL_k$  scheme. For  $Y = (y_1, \dots, y_k) \in E^k$ :

$$(12) \quad s_{t,h}(Y) = z(t+h) \quad \text{for} \quad z' = \alpha_{t,h}(Y)z + \beta_{t,h}(Y), \quad z(t) = y_k.$$

It will be used together with the following Gronwall inequality (see [8, Lemma 196, p.150]). Suppose that  $z(t)$  is a  $C^1$  function and that there exist  $M_1, M_2 > 0$  such that  $|z'(t)| \leq M_1(t - t_0) + M_2$  for all  $t \in [t_0, t_0 + h]$ . Then,

$$(13) \quad \forall t \in [t_0, t_0 + h], \quad |z(t)| \leq e^{M_1(t-t_0)} (|z(t_0)| + M_2(t - t_0)).$$

*Proof of proposition 3.* In this proof it is always assumed that  $0 \leq h, t \leq T$ . We will denote by  $C_i$  a constant only depending on the problem (4) data  $a$  and  $b$  and on  $T$ .

With the assumptions (9) and the definition 1, the function  $\alpha_{t,h}$  is uniformly Lipschitz with a Lipschitz constant  $L_\alpha$ . Moreover we have a uniform bound  $\|\alpha_{t,h}\| \leq M_\alpha$ . Since  $b(t, y)$  is uniformly Lipschitz in  $y$  and since  $0 \leq t \leq T$ , there exists a constant  $K_b$  so that,

$$(14) \quad |b(t, y)| \leq K_b(1 + |y|).$$

Consider the  $RL_3$  scheme,

$$\begin{aligned} |\beta_{t,h}(Y)|_\infty &\leq \frac{11}{3}K_b(1 + |Y|_\infty) + \frac{h}{12}M_a 2K_b(1 + |Y|_\infty) \\ &\leq C_1(1 + |Y|_\infty). \end{aligned}$$

The same inequality holds for the  $RL_2$  and  $RL_4$  schemes. With (12) we have  $s_{t,h}(Y) = z(t+h)$  and,

$$|z'| = |\alpha_{t,h}(Y)z + \beta_{t,h}(Y)| \leq M_\alpha |z| + C_1(1 + |Y|_\infty).$$

The initial state is  $|z(t)| = |y_k| \leq |Y|_\infty$ . With the Gronwall inequality (13) we obtain for  $t \leq \tau \leq t+h$ ,

$$\begin{aligned} |z(\tau)| &\leq e^{M_\alpha h} (|Y|_\infty + hC_1(1 + |Y|_\infty)) \\ &\leq e^{M_\alpha h} (|Y|_\infty(1 + C_1h) + C_1h) \\ (15) \quad &\leq |Y|_\infty(1 + C_2h) + C_2h, \end{aligned}$$

by bounding the exponential with an affine function for  $0 \leq h \leq T$ . This gives the stability condition (11) for  $\tau = t+h$ .

For the  $RL_2$  scheme  $\beta_{t,h}$  is uniformly Lipschitz.

For the  $RL_3$  scheme, consider  $Y = (y_1, y_2, y_3)$  and  $Z = (z_1, z_2, z_3)$  in  $E^3$ . We have,

$$\begin{aligned} |\beta_{t,h}(Y) - \beta_{t,h}(Z)|_\infty &\leq \frac{11}{3}L_b|Y - Z|_\infty + \frac{h}{12} (|a(t, y_3)b(t-h, y_2) - a(t, z_3)b(t-h, z_2)| \\ &\quad + |a(t-h, y_2)b(t, y_3) - a(t-h, z_2)b(t, z_3)|) \end{aligned}$$

Let us bound the Lipschitz constant for a function of the type  $F(Y) = a(\xi, y_2)b(\tau, y_3)$  for  $0 \leq \tau, \xi \leq T$ .

$$\begin{aligned} |F(Y) - F(Z)| &= |a(\xi, y_3)(b(\tau, y_2) - b(\tau, z_2)) + (a(\xi, y_3) - a(\xi, z_3))b(\tau, z_2)| \\ &\leq M_a L_b |Y - Z|_\infty + L_a |Y - Z|_\infty |b(\tau, z_2)|. \end{aligned}$$

With (14), this yields for  $0 \leq \tau, \xi \leq T$  and for  $Y, Z \in E^k$ ,

$$|F(Y) - F(Z)| \leq C_3 |Y - Z|_\infty (1 + |Z|_\infty),$$

As a result,

$$|\beta_{t,h}(Y) - \beta_{t,h}(Z)|_\infty \leq C_4 |Y - Z|_\infty (1 + |Z|_\infty)$$

The same inequality holds for the  $RL_4$  scheme.

Finally consider  $Y_1, Y_2 \in E^k$  and denote  $\alpha_i = \alpha_{t,h}(Y_i)$ ,  $\beta_i = \beta_{t,h}(Y_i)$ . With the property (12),  $s_{t,h}(Y_1) - s_{t,h}(Y_2) = (z_1 - z_2)(t+h)$  where  $z_i$  is the solution to,

$$z_i' = \alpha_i z_i + \beta_i, \quad z_i(t) = Y_{i,k}.$$

On the first hand, with the inequality (15), we have  $|z_2(\tau)| \leq C_5(1 + |Y_2|_\infty)$  for  $t \leq \tau \leq t+h$ .

On the second hand, on  $[t, t + h]$ ,

$$\begin{aligned} |(z_1 - z_2)'| &\leq |\alpha_1||z_1 - z_2| + |\alpha_1 - \alpha_2||z_2| + |\beta_1 - \beta_2| \\ &\leq M_\alpha|z_1 - z_2| + L_\alpha|Y_1 - Y_2|_\infty C_5(1 + |Y_2|_\infty) + C_4|Y_1 - Y_2|_\infty(1 + |Y_2|_\infty) \\ &\leq M_\alpha|z_1 - z_2| + C_6|Y_1 - Y_2|_\infty(1 + |Y_2|_\infty) \end{aligned}$$

The initial condition is  $|(z_1 - z_2)(t)| = |Y_{1,k} - Y_{2,k}| \leq |Y_1 - Y_2|_\infty$ . Then the Gronwall inequality (13) yields,

$$\begin{aligned} |(z_1 - z_2)(t + h)| &\leq e^{M_\alpha h} (|Y_1 - Y_2|_\infty + hC_6|Y_1 - Y_2|_\infty(1 + |Y_2|_\infty)) \\ &\leq e^{M_\alpha h} |Y_1 - Y_2|_\infty (1 + C_6 h(1 + |Y_2|_\infty)). \end{aligned}$$

This last inequality implies the stability condition (10), again by bounding the exponential with an affine function for  $0 \leq h \leq T$ .  $\square$

#### 4. DAHLQUIST STABILITY

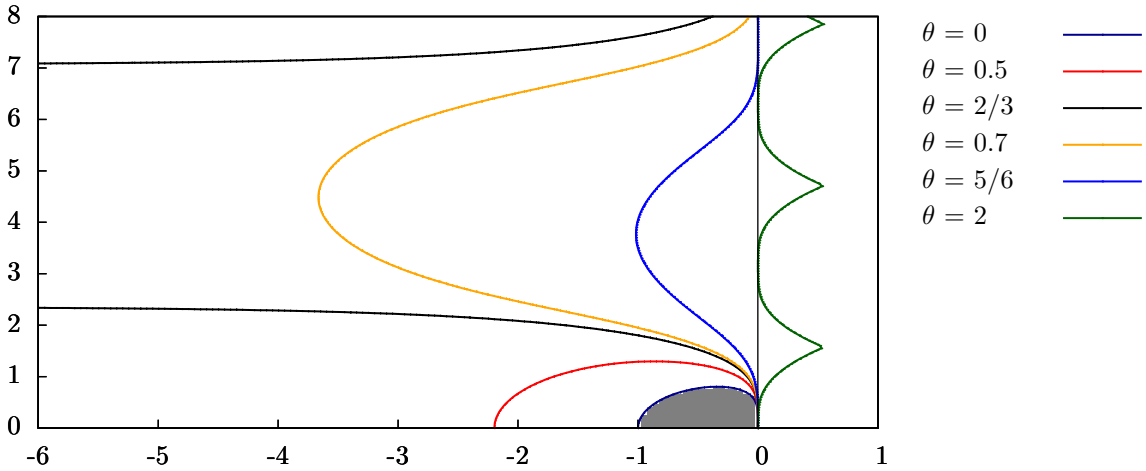


FIGURE 1. Stability domain  $D_\theta$  for the  $RL_2$  scheme for various values of  $\theta$ . The stability domain for the particular case  $\theta = 0$  (no stabilization) is in grey, corresponding to the Adams Bashforth scheme of order 2.

For the general definition concerning the Dahlquist stability we refer to [10]. The background for the Dahlquist stability of exponential integrators with a general varying stabilizer  $a(t, y)$  has been developed in [6], following the ideas of Perego

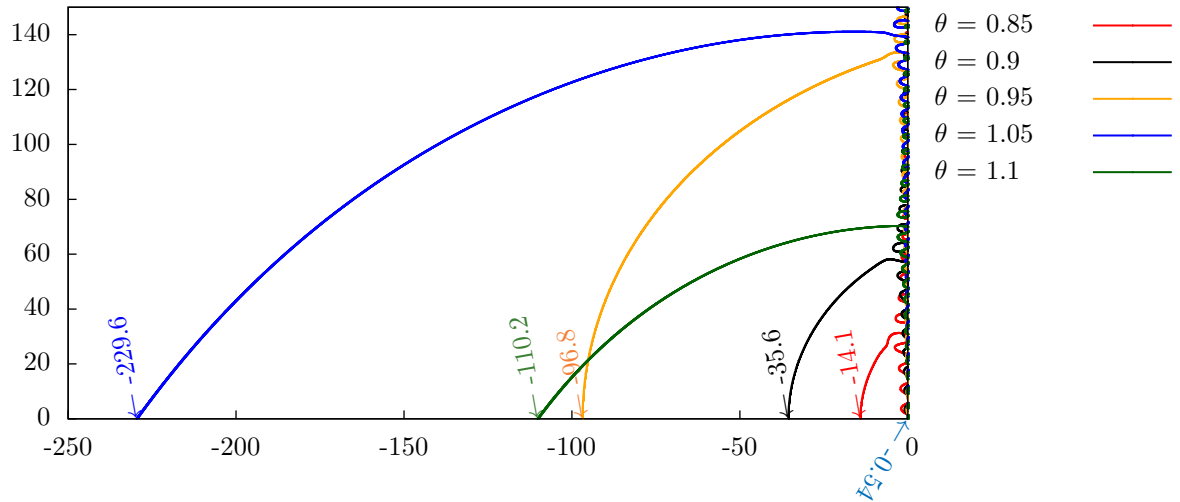


FIGURE 2. Stability domain  $D_\theta$  for the  $RL_3$  scheme. In the particular case  $\theta = 0$  (no stabilization, corresponding to the Adams Bashforth scheme of order 3), the stability domain crosses the  $x$ -axis at  $x \simeq -0.54$  (dark blue arrow).

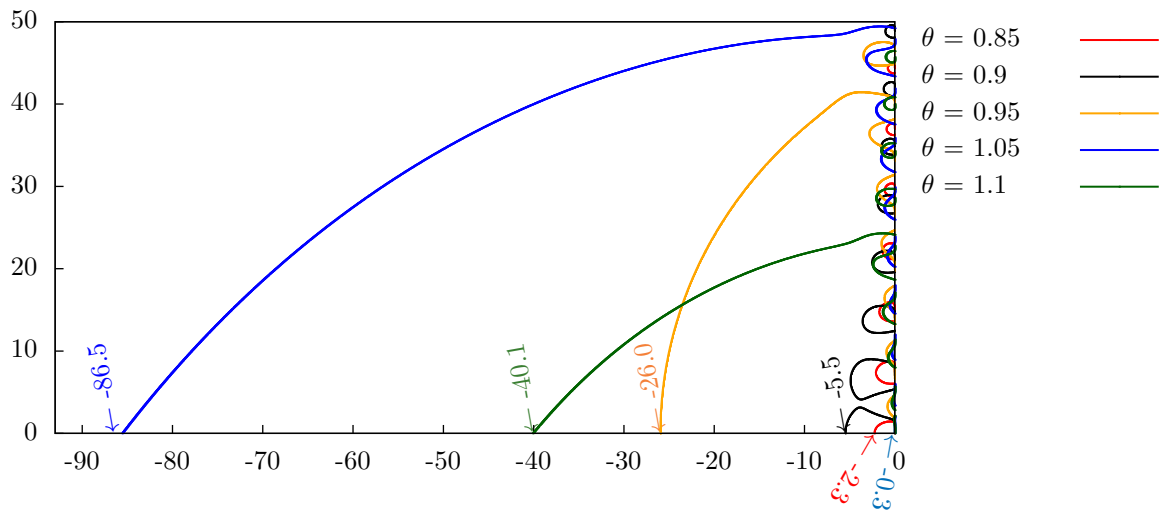


FIGURE 3. Stability domain  $D_\theta$  for the  $RL_4$  scheme. In the particular case  $\theta = 0$  (no stabilization, corresponding to the Adams Bashforth scheme of order 3), the stability domain crosses the  $x$ -axis at  $x \simeq -0.3$  (dark blue arrow).

and Veneziani [24]. Problem (3) is considered with the Dahlquist test function  $f(t, y) = \lambda y$  that is decomposed in (4) as  $f(t, y) = a(t, y)y + b(t, y)$  with,

$$a(t, y) = \theta\lambda, \quad b(t, y) = \lambda(1 - \theta)y.$$

When  $\theta \simeq 1$ , the exact linear part of  $f(t, y)$  in equation (3) is well approximated by  $a(t, y)$ . The stability domain depends on  $\theta$ . It is denoted  $D_\theta$ . At a fixed value of  $\theta$ , it is given by the modulus of a stability function, with the same definition as for multistep methods, see *e.g.* [10]. That stability function has been numerically computed pointwise on a grid inside the complex plane  $\mathbb{C}$ .

*Order 2 Rush Larsen.* The stability domain for the  $RL_2$  scheme has been analyzed in [24]. The situation for this scheme is interesting and we reproduced the results on figure 1.

- If  $0 \leq \theta < 2/3$  the stability domain  $D_\theta$  is bounded. Its size increases with  $\theta$ , starting from the Adams Bashforth scheme of order 2 stability domain when no stabilization occurs ( $\theta = 0$ ).
- If  $\theta = 2/3$ ,  $D_\theta$  contains the negative real axis: the method is  $A(0)$  stable. The domain boundary is asymptotically parallel to the real axis so that the method is not  $A(\alpha)$  stable.
- If  $\theta > 2/3$ , the stability domain is located around the  $y$ -axis: the method is  $A(\alpha)$  stable. The angle  $\alpha$  increases with  $\theta$ , it goes to  $\pi/2$  as  $\theta \rightarrow 1^-$ .

*Rush Larsen of order 3 and 4.* The situation is different for the Rush Larsen methods of order 3 and 4. The stability domains  $D_\theta$  for various values of  $\theta$  have been numerically computed and depicted on figures 2 and 3.

Excepted for the case  $\theta = 1$ , the stability domains are always bounded: the schemes are not  $A$ -stable. However, this stability domain, for values of  $\theta \simeq 1$  are much larger than the  $D_{\theta|_{\theta=0}}$  stability domain when no stabilization occurs ( corresponding to the Adams Bashforth scheme of order 3 or 4). For the order 3 case, the stability domain for  $\theta = 0.85$  is 25 times wider on the left than  $D_{\theta|_{\theta=0}}$ , and for  $\theta = 1.05$  it is 400 times wider. For the order 4 case,  $D_{\theta|_{\theta=1.05}}$  is almost 300 times wider on the left than  $D_{\theta|_{\theta=0}}$ .

## 5. NUMERICAL RESULTS

In this section are presented numerical experiments in order to investigate the performances of the  $RL_k$  method. It will be compared to the exponential integrator of Adams type of order  $k$ 5), shortly denoted  $EAB_k$  here. The  $EAB_k$  schemes have been numerically studied in [6] as compared to several classical methods. It had been shown to be a good candidate for the resolution of the stiff membrane equation in cardiac electrophysiology.

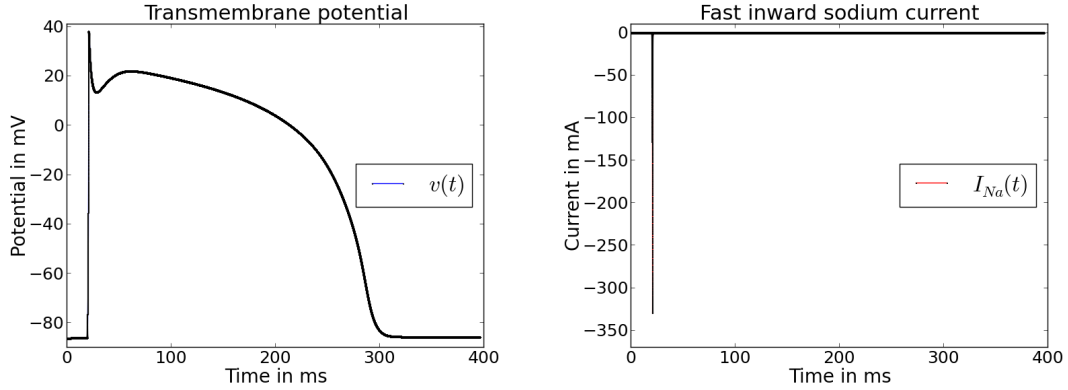


FIGURE 4. *TNNP* model illustration. Left, cellular action potential: starting at a (negative) rest value, the membrane potential  $v(t)$  has a stiff depolarization followed by a plateau and a repolarization to the rest value. Right, depolarization is induced by an ionic sodium current  $I_{Na}$ , with visible stiffness.

**5.1. The membrane equation.** We consider a class of models in cardiac electrophysiology. As illustrated on figure 4, these models display a stiff behaviour characterized by the presence of heterogeneous time scales. The models used to simulate the electrical activity of cardiac cells are ODE systems of the form, see [17, 1, 22, 27]:

$$(16) \quad \begin{aligned} \frac{dw_i}{dt} &= \frac{w_{\infty,i}(v) - w_i}{\tau_i(v)}, & \frac{dc}{dt} &= g(w, c, v), \\ \frac{dv}{dt} &= -I_{ion}(w, c, v) + I_{st}(t), \end{aligned}$$

where  $w = (w_1, \dots, w_p) \in \mathbb{R}^p$  is the vector of the gating variables,  $c \in \mathbb{R}^q$  is a vector of ionic concentrations or other state variables, and  $v \in \mathbb{R}$  is the cell membrane potential. These equations model the evolution of the transmembrane potential of a single cardiac cell. The four functions  $w_{\infty,i}(v)$ ,  $\tau_i(v)$ ,  $g(w, c, v)$  and  $I_{ion}(w, c, v)$  are given reaction terms. They characterize the cell model. The function  $I_{st}(t)$  is a source term. It represents a stimulation current. Problem (16) reformulates into problem (4) form with:

$$(17) \quad a(t, y) = \begin{pmatrix} -1/\tau(v) & 0 & 0 \\ 0 & 0 & 0 \\ 0 & 0 & 0 \end{pmatrix}, \quad b(t, y) = \begin{pmatrix} w_{\infty}(v)/\tau(v) \\ g(y) \\ -I_{ion}(y) + I_{st}(t) \end{pmatrix},$$

for  $y = (w, c, v) \in \mathbb{R}^N$  ( $N = p + q + 1$ ) and where  $-1/\tau(v)$  the  $p \times p$  diagonal matrix with diagonal entries  $(-1/\tau_i(v))_{i=1\dots p}$ . The resulting matrix  $a(t, y)$  is diagonal.

We will consider two such models: the *BeelerReuter* model (BR) [1] or the TNNP model [27] for human cardiac cells.

**5.2. Convergence.** No theoretical solution are available for the chosen application. A reference solution  $y_{ref}$  for a reference time step  $h_{ref}$  is computed with the Runge Kutta 4 scheme to analyze the convergence properties of the  $RL_k$  scheme. Numerical solutions  $y$  are computed to  $y_{ref}$  for coarsest time steps  $h = 2^p h_{ref}$  for increasing  $p$ . Any numerical solution  $y$  consists in successive values  $y_n$  at the time instants  $t_n = nh$ . On every interval  $(t_{3n}, t_{3n+3})$  the polynomial  $\bar{y}$  of degree at most 3 so that  $\bar{y}(t_{3n+i}) = y_{3n+i}$ ,  $i = 0 \dots 4$  is constructed. On  $(0, T)$ ,  $\bar{y}$  is a piecewise continuous polynomial of degree 3. Its values at the reference time instants  $nh_{ref}$  are computed. This provides a projection  $P(y)$  of the numerical solution  $y$  on the reference grid. Then  $P(y)$  can be compared with the reference solution  $y_{ref}$ . The numerical error is defined by,

$$(18) \quad e(h) = \frac{\max |v_{ref} - P(v)|}{\max |v_{ref}|},$$

where the potential  $v$  is the last and stiffest component of  $y$  in equation (16). The

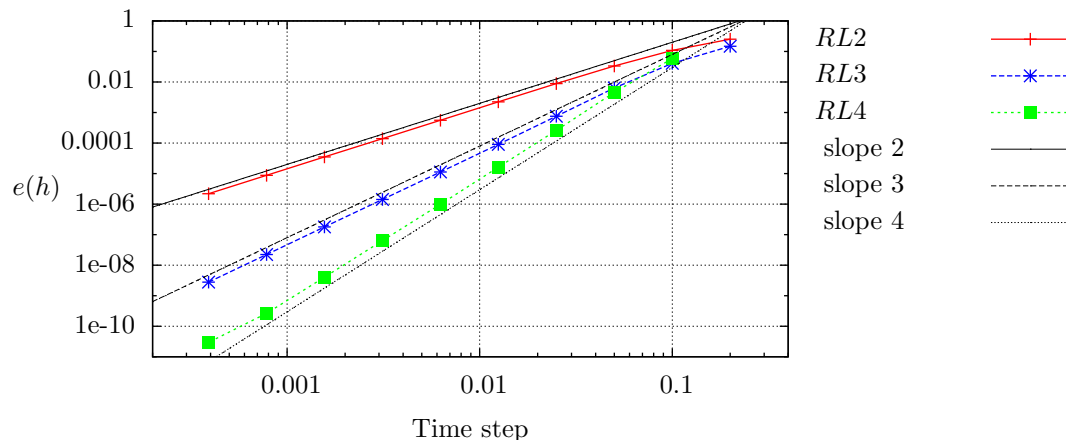


FIGURE 5. Relative error  $e(h)$  (definition (18)) as a function of the time step  $h$  for the  $RL_k$  schemes, for  $k = 2$  to 4 and in Log/Log scale.

numerical convergence graphs for the BR model are plotted on figure 5. All the schemes display the expected asymptotic behaviour  $e(h) = O(h^k)$  as  $h \rightarrow 0$  in corollary 4.

**5.3. Stability robustness to stiffness.** In [26] has been evaluated the stiffness of the BR and TNNP models along one cellular electrical cycle (as depicted on figure 4). The largest negative real part of the eigenvalues of the Jacobian matrix during



this cycle is of  $-1170$  and  $-82$  for the *TNNP* and *BR* models respectively. The *TNNP* model thus is 15 times stiffer than the *BR* model ( $15 \simeq 1170/82$ ).

Robustness to stiffness for the  $RL_k$  scheme is evaluated by comparing the critical time step for these two models. The critical time step  $\Delta t_0$  is defined as the largest time step such that the numerical simulation runs without overflow for  $h < \Delta t_0$ . The results are presented in table 1.

method	$RL_2$	$RL_3$	$RL_4$	$EAB_2$	$EAB_3$	$EAB_4$
BR	0.323	0.200	0.149	0.424	0.203	0.123
TNNP	0.120	0.148	0.111	0.233	0.108	$7.56 \cdot 10^{-2}$

TABLE 1. Critical time step  $\Delta t_0$  for the  $RL_k$  and  $EAB_k$  schemes

An excellent robustness to stiffness can be observed. The critical time step is divided by 2.7, 2.0 and 1.3 for  $k = 2, 3$  and 4 respectively. A comparison with the  $EAB_k$  schemes shows that the two schemes display a robustness to stiffness of same order. For a method that is not  $A(\alpha)$  stable, it is expected for the critical time step to be divided by 15 in case of an increase of stiffness of magnitude 15. This is not observed here, though the  $RL_k$  scheme is not  $A(\alpha)$  stable. The reason for this is that the ODE system (16) is only partially stabilized by (17). Loss of stability is induced by the non-stabilized part, whose eigenvalues are less modified between the *BR* and the *TNNP* models.

**5.4. Accuracy.** The  $RL_k$  scheme is here compared to the  $EAB_k$  scheme in terms of accuracy. This comparison is done by computing the relative error  $e(h)$  in equation (18). The two *BR* and *TNNP* models are considered. We recall that the *TNNP* model is stiffer by a factor 15. The results are collected in the tables 2 and 3.

$h$	$RL_2$	$RL_3$	$RL_4$	$EAB_2$	$EAB_3$	$EAB_4$
0.2	0.251	0.147	-	0.284	0.516	-
0.1	0.107	$4.07 \cdot 10^{-2}$	$5.86 \cdot 10^{-2}$	$9.26 \cdot 10^{-2}$	$9.17 \cdot 10^{-2}$	0.119
0.05	$3.35 \cdot 10^{-2}$	$6.34 \cdot 10^{-3}$	$4.58 \cdot 10^{-3}$	$2.31 \cdot 10^{-2}$	$1.09 \cdot 10^{-2}$	$8.96 \cdot 10^{-3}$
0.025	$8.88 \cdot 10^{-3}$	$7.57 \cdot 10^{-4}$	$2.61 \cdot 10^{-4}$	$5.39 \cdot 10^{-3}$	$1.17 \cdot 10^{-3}$	$4.33 \cdot 10^{-4}$

TABLE 2. Relative error  $e(h)$  (eq. (18)) for the *BR* model.

For the  $RL_2$  and the  $EAB_2$  schemes, the accuracies are very close, the  $EAB_2$  scheme being slightly more accurate for the *BR* model. For the orders 3 and 4, a non negligible difference is observed between the *RL* and *EAB* schemes. The *RL* scheme is more accurate at large time steps. For smaller time steps, accuracies are almost

$h$	$RL_2$	$RL_3$	$RL_4$	$EAB_2$	$EAB_3$	$EAB_4$
0.1	0.177	0.305	0.421	0.351	0.530	-
0.05	$7.39 \cdot 10^{-2}$	$4.54 \cdot 10^{-2}$	$4.61 \cdot 10^{-2}$	$9.01 \cdot 10^{-2}$	$5.59 \cdot 10^{-2}$	$8.93 \cdot 10^{-2}$
0.025	$2.21 \cdot 10^{-2}$	$6.53 \cdot 10^{-3}$	$5.96 \cdot 10^{-3}$	$2.14 \cdot 10^{-2}$	$7.34 \cdot 10^{-3}$	$8.34 \cdot 10^{-3}$
0.0125	$5.75 \cdot 10^{-3}$	$8.05 \cdot 10^{-4}$	$3.21 \cdot 10^{-4}$	$5.11 \cdot 10^{-3}$	$7.62 \cdot 10^{-4}$	$3.70 \cdot 10^{-4}$

TABLE 3. Relative error  $e(h)$  (eq. (18)) for the  $TNNP$  model.

the same. This means that  $RL$  and  $EAB$  schemes are equivalent in terms of accuracy considering the asymptotic convergence region, but outside this region,  $RL$  scheme is more precise.

## 6. CONCLUSION

We introduced in this paper two new ODE solvers that we named Rush Larsen of order 3 and 4. They are explicit multistep exponential integrators. Their general definition (7) is very simple inducing an easy implementation. We provided a convergence and stability under perturbation analysis of these two schemes. We also performed their Dahlquist stability analysis: they are not  $A(0)$  stable but display a very large stability domain for sufficiently precise stabilization. The numerical properties of the schemes are analyzed for a complex and realistic stiff application. The  $RL_k$  schemes are as stable as exponential integrators of Adams type, allowing simulations at large time step. The  $RL_k$  schemes moreover are more accurate for  $k = 3$  and 4 when considering large time steps. They are shown to be robust to stiffness both in terms of stability and of accuracy.

## REFERENCES

- [1] G.W. Beeler and H Reuter. Reconstruction of the Action Potential of Ventricular Myocardial Fibres. *J. Physiol.*, 268:177–210, 1977.
- [2] M. T. Chu. An automatic multistep method for solving stiff initial value problems. *J. Comput. Appl. Math.*, 9(3):229–238, 1983.
- [3] J.C. Clements, J. Nenonen, P.K. Li, and B.M. Horacek. Activation dynamics in anisotropic cardiac tissue via decoupling. *Ann. Biomed. Eng.*, 32(7):984–990, 2004.
- [4] P. Colli-Franzone, L.F. Pavarino, and B. Taccardi. Monodomain simulations of excitation and recovery in cardiac blocks with intramural heterogeneity. in *Functional Imaging and Modeling of the Heart (FIMH05)*, *Lect. Notes Comput. Sci.*, 3504:267–277, 2005.
- [5] P. Colli-Franzone, L.F. Pavarino, and B. Taccardi. Simulating patterns of excitation, repolarization and action potential duration with cardiac Bidomain and Monodomain models. *To appear in Math. Biosci.*, 2005.
- [6] Y. Coudière, C. Douanla Lontsi, and C. Pierre. Exponential Adams Bashforth integrators for stiff ODEs, application to cardiac electrophysiology. *HAL Preprint*, 2016.

- [7] S. M. Cox and P. C. Matthews. Exponential time differencing for stiff systems. *J. Comput. Phys.*, 176(2):430–455, 2002.
- [8] Sever Silvestru Dragomir. *Some Gronwall type inequalities and applications*. Nova Science Publishers, Inc., Hauppauge, NY, 2003.
- [9] E. Hairer, S. P. Nørsett, and G. Wanner. *Solving ordinary differential equations. I*, volume 8 of *Springer Series in Computational Mathematics*. Springer-Verlag, Berlin, 1993.
- [10] E. Hairer and G. Wanner. *Solving ordinary differential equations. II*, volume 14 of *Springer Series in Computational Mathematics*. Springer-Verlag, Berlin, 2010.
- [11] M. Hochbruck and A. Ostermann. Explicit Exponential Runge-Kutta Methods for Semilinear Parabolic Problems. *SIAM J. Numerical Analysis*, 43(3):1069–1090, 2005.
- [12] Marlis Hochbruck. A short course on exponential integrators. In *Matrix functions and matrix equations*, volume 19 of *Ser. Contemp. Appl. Math. CAM*, pages 28–49. Higher Ed. Press, Beijing, 2015.
- [13] Marlis Hochbruck, Christian Lubich, and Hubert Selhofer. Exponential integrators for large systems of differential equations. *SIAM J. Sci. Comput.*, 19(5):1552–1574 (electronic), 1998.
- [14] Marlis Hochbruck and Alexander Ostermann. Exponential integrators. *Acta Numer.*, 19:209–286, 2010.
- [15] Marlis Hochbruck and Alexander Ostermann. Exponential multistep methods of Adams-type. *BIT*, 51(4):889–908, 2011.
- [16] Marlis Hochbruck, Alexander Ostermann, and Julia Schweitzer. Exponential Rosenbrock-type methods. *SIAM J. Numer. Anal.*, 47(1):786–803, 2008/09.
- [17] A.L. Hodgkin and A.F. Huxley. A quantitative description of membrane current and its application to conduction and excitation in nerve. *J. Physiol.*, 117:500–544, 1952.
- [18] Antti Koskela and Alexander Ostermann. Exponential Taylor methods: analysis and implementation. *Comput. Math. Appl.*, 65(3):487–499, 2013.
- [19] D. Lee and S. Preiser. A class of non linear multistep A-stable numerical methods for solving stiff differential equations. *Comp. & maths with appls.*, 4:43–51, 1978.
- [20] V. T. Luan and A. Ostermann. Explicit exponential runge kutta methods of high order for parabolic problems. *J. Comput. Appl. Math.*, 256:168–179, 2014.
- [21] C.H. Luo and Y. Rudy. A model of the Ventricular Cardiac Action Potential. *Circ. Res.*, 68:1501–1526, 1991.
- [22] C.H. Luo and Y. Rudy. A Dynamic Model of the Cardiac Ventricular Action Potential I. Simulations of Ionic Currents and Concentration Changes. *Circ. Res.*, 74:1071–1096, 1994.
- [23] B.V. Minchev and W. M. Wright. A review of exponential integrators for first order semi-linear problems. Technical report, Norwegian university of science and technology trondheim, 2005.
- [24] M. Perego and A. Veneziani. An efficient generalization of the Rush-Larsen method for solving electro-physiology membrane equations. *ETNA*, 35:234–256, 2009.
- [25] G. Rainwater and M. Tokman. A new class of split exponential propagation iterative methods of Runge-Kutta type (sEPIRK) for semilinear systems of ODEs. *J. Comput. Phys.*, 269:40–60, 2014.
- [26] R. J. Spiteri and C. D. Ryan. Stiffness Analysis of Cardiac Electrophysiological Models. *Annals of Biomedical Engineering*, 38:3592–3604, Dec 2010.
- [27] K.H. Ten Tusscher, D. Noble, P.J. Noble, and A.V. Panfilov. A Model for Human Ventricular Tissue. *Am J Physiol Heart Circ Physiol*, 286, 2004.
- [28] M. Tokman, J. Loffeld, and P. Tranquilli. New adaptive exponential propagation iterative methods of Runge-Kutta type. *SIAM J. Sci. Comput.*, 34(5):A2650–A2669, 2012.

- [29] Paul Tranquilli and Adrian Sandu. Rosenbrock-Krylov methods for large systems of differential equations. *SIAM J. Sci. Comput.*, 36(3):A1313–A1338, 2014.

YVES COUDIÈRE, INRIA BORDEAUX SUD OUEST, UNIVERSITÉ DE BORDEAUX  
*E-mail address:* `yves.coudiere@inria.fr`

CHARLIE DOUANLA LONTSI, INRIA BORDEAUX SUD OUEST, UNIVERSITÉ DE BORDEAUX  
*E-mail address:* `charlie.douanla-lontsi@inria.fr`

CHARLES PIERRE, CNRS, UNIVERSITÉ DE PAU, LMAP  
*E-mail address:* `charles.pierre@univ-pau.fr`